

# FDS Verification Supplement - 2D Vortex Simulation

Max Gould  
*NIST, Gaithersburg, MD 20899*  
(Dated: August 03, 2012)

## 2D VORTEX SIMULATION

In this section we present another case that demonstrates the second-order accuracy of the FDS transport algorithm. We consider the analytically stable flow field consisting of a single vortex advected by a uniform flow, a test case developed by CERFACS. Maintaining the geometry of the vortex over time provides a good measure of the order of accuracy of the transport scheme.

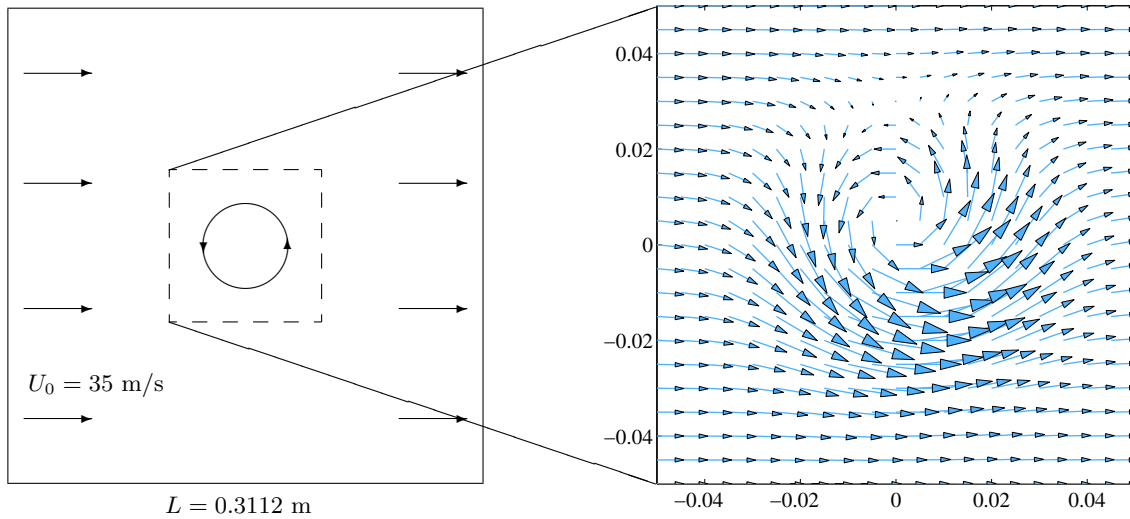


FIG. 1. Vector field of a two-dimensional vortex in a constant flow field.

The vortex is initially defined as the gradient of the potential field,

$$\Psi_0(x, z) = \Gamma \exp\left[-\frac{x^2 + z^2}{2 R_c^2}\right], \quad (1)$$

where  $\Gamma$  determines its intensity and  $R_c$  its characteristic size. The velocity components are determined by taking the gradient of the potential field superimposed on the constant flow field of velocity  $U_0$  in the positive  $x$  direction,

$$u(x, z) \equiv U_0 + \frac{\partial}{\partial z} \Psi_0 = U_0 - \frac{\Gamma z}{R_c^2} \exp\left[-\frac{x^2 + z^2}{2 R_c^2}\right], \quad (2)$$

$$w(x, z) \equiv -\frac{\partial}{\partial x} \Psi_0 = \frac{\Gamma x}{R_c^2} \exp\left[-\frac{x^2 + z^2}{2 R_c^2}\right], \quad (3)$$

where  $u$  and  $w$  refer to velocity in the  $x$  and  $z$ -directions, respectively. For our purposes we need only analyze one component of the velocity field. We will focus our attention on the  $u$ -component of velocity.

We define the computational domain as a two-dimensional square region,  $L = 0.3112$  m on a side, with periodic boundary conditions. The domain is discretized for a range of square, two-dimensional meshes of  $40^2$ ,  $80^2$ ,  $160^2$ , and  $320^2$  grid cells. For the purposes of this test, we set the flow parameters as

$$\begin{aligned} U_0 &= 35 \text{ m/s} \\ R_c &= L/20 = 0.01556 \text{ m} \\ \Gamma &= 0.04 U_0 R_c \sqrt{e} = 0.0359157 \end{aligned}$$

The constant flow field and periodic boundary conditions cause the vortex to repeatedly pass through the computational domain. The “pass-through” time,  $t_f$ , is defined as the time period required for the stable vortex to return to its original position,

$$t_f = L/U_0 \simeq 8.8914 \times 10^{-3} \text{ s.}$$

To ensure that the numerical solution converges to the analytical solution, we set the time step,  $dt$ , so that the Courant-Friedrichs-Lewy (CFL) number is 0.5.

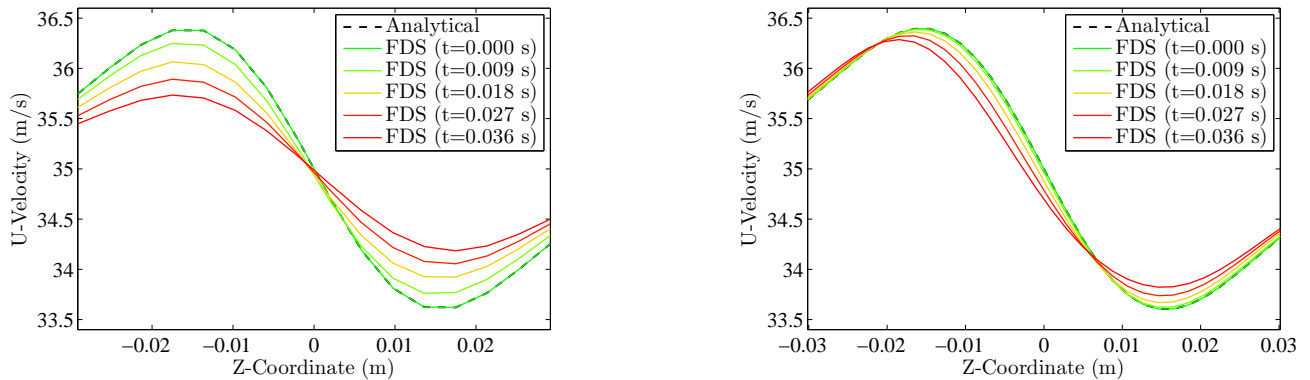


FIG. 2.  $u$ -velocity along the  $z$ -axis at  $x = 0$  plotted for each of the vortex's first four loops through the computational domain. (Left)  $80^2$  grid cell model. (Right)  $160^2$  grid cell model.

A plot of  $u$ -velocity values just along the  $z$ -axis provides a simple characterization of the vortex geometry. The extent to which this geometry changes over time provides a qualitative measure of the accuracy of the transport algorithm. Figure 2 displays these plots for two different grid resolutions. Each line represents a plot taken for a different number of flow-through times such that the red lines represent the vortex after it has undergone the most passes through the computational domain while the green lines represent the vortex in the initial phase. The broken black line represents the analytical solution. As the vortex undergoes more passes through the computational domain, its velocity profile diverges further and further from the analytical profile. While divergence still occurs on the finer mesh, the extent to which it diverges after the same number of flow-through times is significantly smaller.

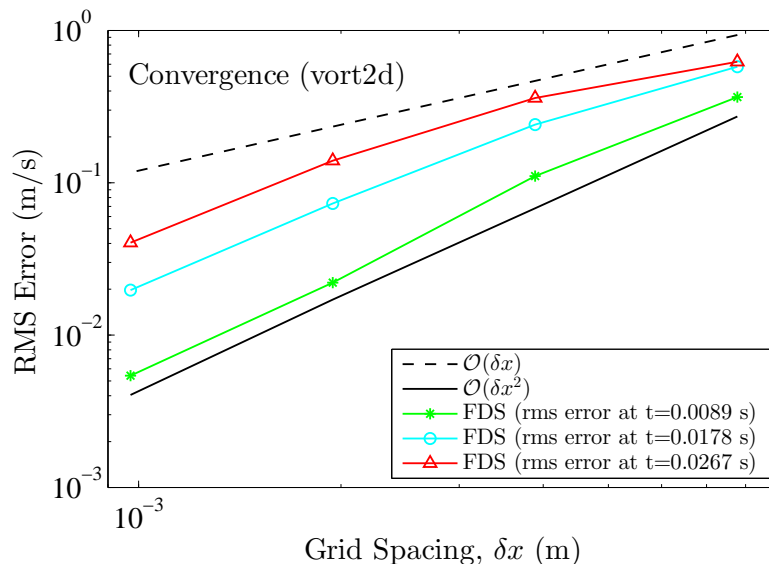


FIG. 3. Rms error between simulated and analytical  $u$ -velocity values along the  $z$ -axis plotted for each grid resolution at each of three subsequent passes of the vortex through the computational domain.

The rate with which the simulated profiles converge to the analytical one defines the order of accuracy of the numerical scheme. In Figure 3 we plot the rms error of the numerical solution as a function of the grid resolution. The three colored curves represent the rms error at three different pass-through times. The broken and solid black lines represent the plot gradient corresponding to first and second order error respectively. While the error increases with each flow-through time, the gradients of the lines are roughly parallel to the solid black line, indicating second-order accuracy of the numerical scheme.

To analyze the stability of the vortex at times other than discrete multiples of the pass-through time, consider the time-dependent potential field and its corresponding  $u$ -velocity component:

$$\Psi(x, z, t) = \Psi_0 \exp \left[ \frac{2 U_0 x t - U_0^2 t^2}{2 R_c^2} \right], \quad (4)$$

$$u(x, z, t) = U_0 - \Psi_0 \frac{z}{R_c^2} \exp \left[ \frac{2 U_0 x t - U_0^2 t^2}{2 R_c^2} \right]. \quad (5)$$

In Figure 4, we show the  $u$ -velocity at a single point, on the lower left fringe of the vortex, for two different mesh resolutions,  $80^2$  and  $160^2$ . A mesh resolution of  $320^2$  grid cells produces a plot that is, to the eye, a perfect match out to four pass-through times.

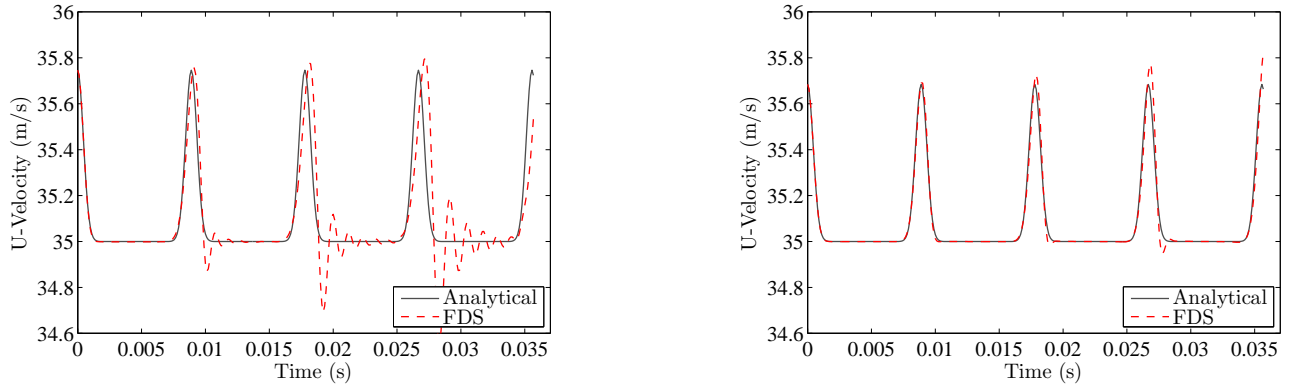


FIG. 4. Simulated and analytical values of  $u$ -velocity at a point plotted as a function of time over a time period equal to four times the flow-through time. (Left)  $80^2$  grid cell model. (Right)  $160^2$  grid cell model.